Energy Reports 7 (2021) 6148–6161

Contents lists available at ScienceDirect

Energy Reports

journal homepage: www.elsevier.com/locate/egyr

Research paper

Frequency stability of the Israeli power grid with high penetration of renewable sources and energy storage systems

Gefen Ben Yosef [a,*], Aviad Navon [a], Olga Poliak [b], Naomi Etzion [b], Nurit Gal [c], Juri Belikov [d], Yoash Levron [a]

[a] Andrew and Erna Viterbi Faculty of Electrical Engineering Technion—Israel Institute of Technology, Haifa 3200003, Israel
[b] Planning Development and Technology Division, Israel Electric Corporation Ltd., POB 10, Haifa 3100, Israel
[c] School of Business Administration, The Hebrew University, Jerusalem, 9190501, Israel
[d] Department of Software Science, Tallinn University of Technology, Akadeemia tee 15a, 12618 Tallinn, Estonia

ARTICLE INFO

Article history:
Received 30 May 2021
Received in revised form 5 September 2021
Accepted 13 September 2021
Available online xxxx

Keywords:
Renewable energy
Geographical distribution
Frequency stability
Energy storage

ABSTRACT

As countries worldwide are integrating more energy storage systems and renewable energy sources, it is important to examine how these impact the frequency stability of the grid. In this study we explore this question by focusing on Israel in 2025. Based on the Israeli power grid model in 2025, which includes detailed information on the entire transmission network, generation units, and loads, we examine hundreds of different locations and sizes of renewable energy sources and energy storage systems, focusing on the frequency behavior in each scenario following the loss of a large generator. This is done using the industry-standard PSS/E simulator. The results lead to several design-level recommendations. One main conclusion is that the Israeli power system already has the required resources to maintain frequency stability in case a large generation unit is lost. However, to maintain a reliable system, policy makers should encourage that the existing and additional storage will contribute to frequency regulation when there is a risk of instability. We also find that the location of renewable energy sources and energy storage systems has an impact on the frequency stability, and that it is better to place storage systems in the south, and renewable energy sources in the north. However, at least until 2025 this impact is not yet strong enough to be a leading factor in determining the location of these sources.

1. Introduction

Large-scale integration of renewable energy sources (RES) poses significant challenges (Liang, 2017; Ulbig et al., 2014; Hirth and Ziegenhagen, 2015), one of them is maintaining a balance between generation and consumption of energy at all times. This balance is relatively easy to achieve with conventional generation units, but is harder to maintain with RES, due to their intermittent nature. In addition, unlike conventional generation units, most renewable sources do not provide inertia, which is critical for regulating the system frequency (Ulbig et al., 2014; Milano et al., 2018). If the inertia is too low then imbalances between generation and consumption may result in high frequency deviations, which can trip protection systems, and eventually lead to a blackout.

Several studies demonstrate the impact of RES on the system frequency and overall dynamics (Mentesidi et al., 2016; Wu et al., 2013; Alquthami et al., 2010; Wu et al., 2016; Remon et al., 2017; Abdlrahem et al., 2013; Liu et al., 2018; Kottick et al., 1991). A repeating conclusion is that a high share of renewable energy generation poses a risk to the system's stability. For instance, Wu et al. (2013) use Kinmen Island as a case study, and show that increased photovoltaic (PV) penetration increases the magnitude of frequency oscillations under three types of events: changing solar irradiance, PV generation losses, and short circuit faults. The same events are examined by Alquthami et al. (2010), who use the 39-bus 5620 MW New England test-case system to examine its dynamics when additional PV generation is distributed between three large PV plants. The results show that at 20% penetration level frequency deviations might trigger load shedding. Another study examines the three main interconnections in the U.S. Liu et al. (2018). The authors simulate the loss of generation units, and examine the resulting frequency response. It is found that when the penetration level of PV sources increases then frequency stability is adversely affected, where the largest effect is measured in the smallest interconnection. In addition, Seneviratne and Ozansoy (2016) list several additional studies that demonstrate the adverse impact of wind and PV

* Corresponding author.
E-mail address: gefenb@protonmail.com (G.B. Yosef).

https://doi.org/10.1016/j.egyr.2021.09.057

List of abbreviations

BESS	Battery energy storage system
DRES	Distributed renewable energy sources
ESS	Energy storage systems
IECo	Israeli electric corporation
PHS	Pumped hydro storage
PSS/E	Power system simulator for engineering
PV	Photovoltaic
RES	Renewable energy sources
SNSP	System non-synchronous penetration ratio
TSO	Transmission system operator
UC	Unit commitment
URES	Utility-scale renewable energy sources

penetration on the frequency stability, following the loss of a large generator.

Energy storage systems (ESS) are recognized as a tool to improve frequency stability by different means, such as virtual inertia, and numerous studies examine ESS optimal siting and sizing to improve the frequency stability. Several studies analyze the optimal placement of virtual inertia (Poolla et al., 2017, 2019), concluding that frequency stability is determined not only by the total inertia in the system, but also by the location of the power disturbance and the placement of the additional inertia in the grid. Another conclusion is that in order to mitigate the most severe disturbance, ESS should be placed such that the inertia is equal at all buses. A similar conclusion is derived by Silva-Saravia et al. (2017), who examine the optimal location of flywheels for primary frequency regulation and inter-area oscillations damping. The results, later verified in simulation, point out that the best locations for mitigating inter-area oscillations are in areas with "low density" of inertia. The same conclusion is derived in another study, in which the impact of the location of electronically-interfaced resources, with either damping or inertia emulating controllers, is examined (Pulgar-Painemal et al., 2018). However, contrary to the studies above that suggest to place ESS such that the inertia will be more evenly distributed, other studies find that ESS is better placed in specific locations. For instance, Adrees and Milanovic (2016) examine the impact of bulk vs. distributed ESS on frequency stability. The study finds that at higher PV penetration levels a single large storage offers superior frequency support, in comparison to distributed storage. Another study, based on a case study of a fault in the IEEE 9-bus power system, finds that it is better to place virtual inertia close to the synchronous generator which operates in a steady-state condition (Cheema and Mehmood, 2020). Finally, two comprehensive surveys explore hundreds of studies that examine optimal allocation of distributed generation (Singh and Mishra, 2018; Bawazir and Cetin, 2020). The majority of the surveyed studies target issues such as line capacity, voltage stability, power loses, and operational costs.

The state of Israel, like other countries worldwide, set targets for the integration of RES. In 2015 the targets included generation of 13% of the annual electrical energy by RES until 2025, and generation of 17% by 2030 (Israel Prime Ministers Office, 2015). The target for 2030 was recently updated to 30%, but the target for 2025 was not updated accordingly (Israel Ministry of Energy, 2020). Although in 2019 RES accounted for only 5% of the annual electrical energy (Israel Electric Authority, 2019), later in the spring of 2020, during the COVID-19 pandemic, the share of RES in the instantaneous power generation reached 29% at certain times. This high share of RES during the pandemic introduced stability challenges, which provided a glimpse to a renewable rich future. Some of these challenges are studied by Carmon et al. (2020) who examine the effect of the high share of RES during the pandemic on the Israeli grid, and conclude that a main challenge was frequency regulation. The shift to even higher shares of RES will further increase existing technical challenges, and is expected to create new ones.

In view of these challenges, several recent works study the integration of RES and energy storage systems in the Israeli power grid (Vardimon, 2011; Kottick et al., 1993; Halász and Malachi, 2014; Solomon et al., 2010, 2012a,b, 2019; Bogdanov and Breyer, 2015; Navon et al., 2020). For instance, Vardimon (2011) assesses the potential of distributed PV and finds that rooftop PV alone can account for 32% of the yearly national electric energy consumption already in 2008. Halász and Malachi (2014) propose an irradiation fluctuation rank for different sites suitable for PV installations in the Israeli desert. The motivation is to suggest where to place future PV power plants such that power and frequency fluctuations are minimized. Solomon et al. (2010, 2012a,b) study PV integration in Israel by examining the Israeli power grid as an isolated grid, while using hourly data of conventional generation, solar generation, and demand. One conclusion is that increasing the variability of the generated power in conventional generators may support future integration of renewable source. Navon et al. (2020) examine how integration of RES affects the load in transmission lines. The study concludes that transmission line congestion inhibits renewable energy integration, and that line loads can be significantly relieved by optimal distribution of solar power plants. Kottick et al. (1993) simulate the effects of a 30 MW battery energy storage system (BESS) on the frequency in the Israeli grid, following a sudden variation in the load, and show that BESS can drastically reduce frequency deviations. Studies for other countries for the integration of RES and energy storage systems can be found for instance in Tahir et al. (2019a,b).

In comparison to the recent works surveyed above, in this study we explore how the location and size of renewable energy sources and energy storage systems impact the frequency stability of the grid, as we focus on Israel in 2025, using the most realistic dynamic model available. Through this exploration we wish to contribute new ideas and insights to other researchers and policy makers regarding this highly important question. Based on the Israeli grid model, which includes detailed information on the entire transmission network, generation units, and loads, we examine hundreds of different locations and sizes of renewable energy sources and energy storage systems, focusing on the frequency behavior in each scenario following the loss of a large generator. The work has been done in collaboration with the Israeli Electric Corporation (IECo) using their most updated databases, and the results have been thoroughly tested and discussed by leading power system dynamics experts in Israel. The refined set of results allow us to suggest several policy recommendations for the siting and sizing of energy storage systems and renewable energy sources in Israel.[1] One main conclusion is that the Israeli power system already has the required resources to maintain a stable frequency in case a large generation unit is lost. However, to maintain a reliable system, policy makers should consider actions that will ensure that the existing and additional storage will contribute to the frequency regulation when there is a risk of instability. In addition, we demonstrate that storage requirements may decrease as the renewable energy penetration level increases, and that the marginal contribution of storage for frequency regulation decreases as the overall power

[1] This study was done as part of the first author's MSc degree, and presents only the professional opinion of the authors.

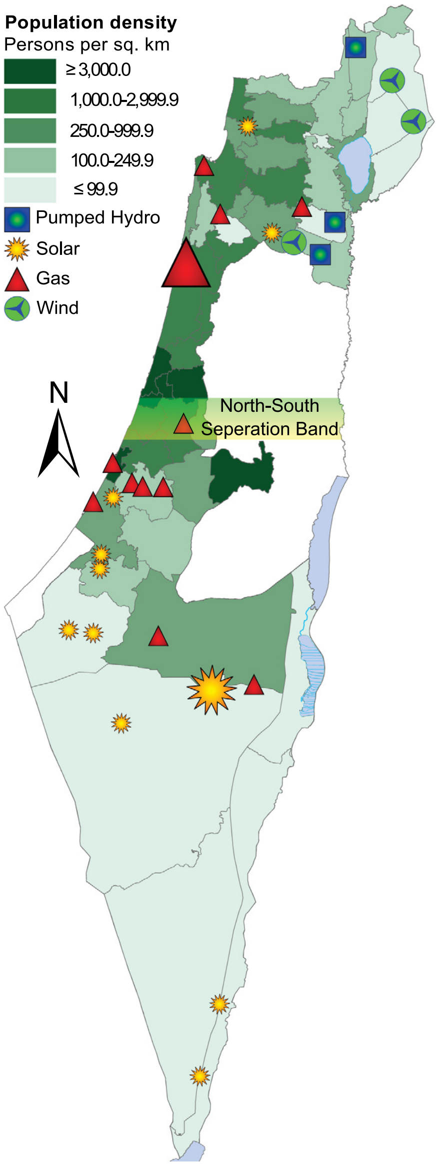

Fig. 1. The expected Israeli power system in 2025. The largest conventional generation unit and renewable energy plant are marked with larger icons.

capacity of storage increases. Moreover, we suggest a measure that indicates how the distribution of storage may affect energy curtailment at buses that contain both renewable energy sources and storage systems. We also find that the location of renewable energy sources and energy storage systems has an impact on the frequency stability, and their preferred location seems to balance the distribution of inertia in the Israeli grid. However, this impact is not yet strong enough to be a leading factor in determining the location of these sources at least until 2025.

The paper continues as follows. Section 2 provides background on the Israeli grid and its frequency control mechanisms. Section 3 explains methods used in this work. Section 4 attempts to find what are the optimal distributions of generation units and storage for frequency stability. Section 5 examines what are the minimum storage requirements to handle the worst-case generation loss in Israel, for different renewable energy penetration targets. Section 6 concludes the paper.

2. Background

2.1. Frequency control in Israel

Frequency control in the Israeli grid is essentially the same as in most power systems worldwide. The control relies mainly on spinning reserves, the flexibility of online generation units, and the inertia of large synchronous machines. Following an event such as a fault, or the loss of a large generation unit, the inertia of the synchronous machines is immediately restricting the frequency rate-of-change. Shortly after that, online units that have spinning reserves respond in a matter of seconds to provide more power, and restrain the frequency deviation. In case of extreme deviations, for example when the frequency falls below 49 Hz, under-frequency load shedding is executed. Lastly, in a process that takes 15 to 30 min, more power is dispatched to online units, and offline units are turned on if needed.

The Transmission System Operator (TSO) in Israel has limited ability to handle frequency deviations due to several factors: lack of regulations that target spinning reserve, the isolated nature of the system, gas supply security, coal environmental restrictions, and economical considerations. In addition, Israel has a mix of coal units, gas units, gas turbines, and jet turbines, which all have very different technical properties. The steam units (coal or gas) have long initiation times and thus are used for base load generation, since they cannot be shutdown and turned-on daily. On the other hand, the gas and jet turbines have short response times, and so can be shut-down and turned-on daily. During seasons of low demand, when the share of solar generation increases, several coal units may be shut-down in order to operate smaller and more flexible gas and jet units, which can mitigate the intermittency of solar generation and regulate the frequency. This mode of operation is less economical but is required in order to operate the power system more reliably. In the near future several jet turbines, which provide flexibility, are planned to be closed. Moreover, demand side management, as a flexible tool for frequency regulation, is very limited in Israel, and is mainly based on load shedding.

The only utility-scale energy storage system in Israel, as of 2021, is a single Pumped Hydro Storage (PHS) system, rated at 300 MW (Shikun Binui, Electra, 2016). This system helps operators to regulate the frequency during times of low demand and high solar generation, by acting as a load. While acting as a load the storage allows to activate more conventional units, which provide flexibility and inertia, and also provides a large controllable unit that may be shed in case of extreme frequency deviations. It should be noted that the ratio between energy capacity to power capacity in PHS storage systems is relatively high, and therefore this technology is more suitable for other applications, such as energy shifting.

2.2. The Israeli grid

The Israeli grid is divided very distinctively between north and south. The map of the Israeli grid in 2025, shown in Fig. 1, illustrates this division very well. In this map the ground layer illustrates the population density in 2018 (Israel Central Bureau of Statistics, 2019), which correlates well with the distribution of load in Israel due to the low amount of heavy industries. As can be seen in the map most of the population, and thus also the load, is in the north. The map also marks the locations of the main conventional generators, pumped hydro storage systems, wind farms, and solar plants. The location of the largest conventional generation unit, which is in the north, and the largest renewable energy plant, which is in the south, are marked with larger icons. It can be noticed that all pumped hydro storage systems and

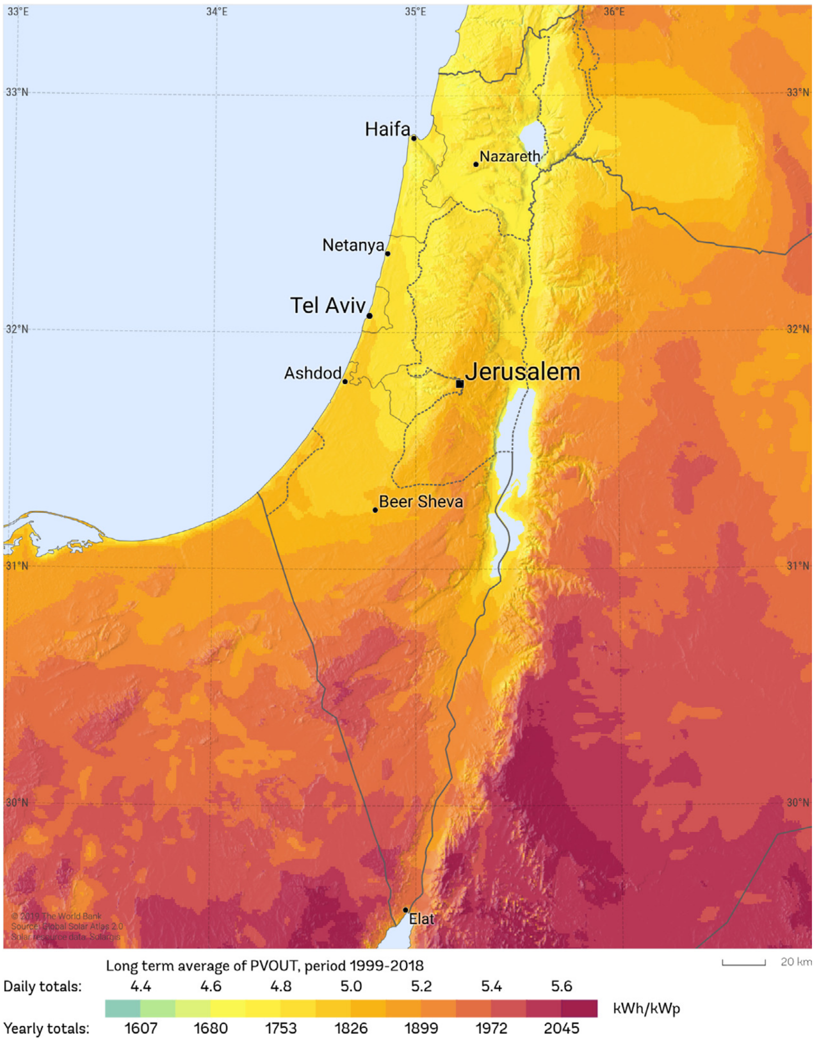

Fig. 2. Photovoltaic power potential in Israel. *Source:* Global Solar Atlas 2.0, Solar resource data: Solargis
© 2019 The World Bank.

Table 1
Total power generation capacities in Israel in 2025 [MW].

Type of unit	North	South
Conventional	7300	10 800
Utility-scale RES (URES)	490	1310
Distributed RES (DRES)	850	1540

Table 2
Dynamic models used in this work, as named in PSS/E (Siemens PTI, 2010).

System component	Model
Synchronous units	GENROU/GENSAL generator models TGOV5/GAST/GAST2A turbine-governor models IEE2ST stabilizer model Various excitation system models
Utility-scale RES	REGCAU1 renewable energy generator/converter model REECBU1 electrical control model for large scale PV
Storage systems	LDSHXX under-frequency load shedding model with 2 activation levels at 49.5 and 49.3 Hz
Load characteristic	LDFRAL load–frequency model

major wind farms are located in the north, while most of the conventional generation and almost all major solar plants are located in the south. The high solar capacity in the south is due to the high PV potential in this area, as seen in Fig. 2, as well as the low-cost and available land there (Israel Government Portal, 2017).

Table 1 summarizes the total generation capabilities in Israel in 2025, categorized by the type of unit.[2] The largest renewable energy plant that is expected to operate by 2025 is a 500 MW PV plant in the south of Israel, and the largest generation unit is a 650 MW combined-cycle gas turbine in the north. Other significant facilities that are expected to operate in 2025 are three pumped hydro storage systems with a total capacity of 800 MW (Israel Electric Authority, 2020c). Moreover, at least 168 MW of distributed PV plus storage will be connected until 2025. However, currently there is no regulation that incentivizes their contribution to frequency regulation (Israel Electric Authority, 2020b).

2 The amount of renewable energy sources is estimated based on existing connection requests. In practice, in order to reach the target for 2025, the total amount is expected to be higher.

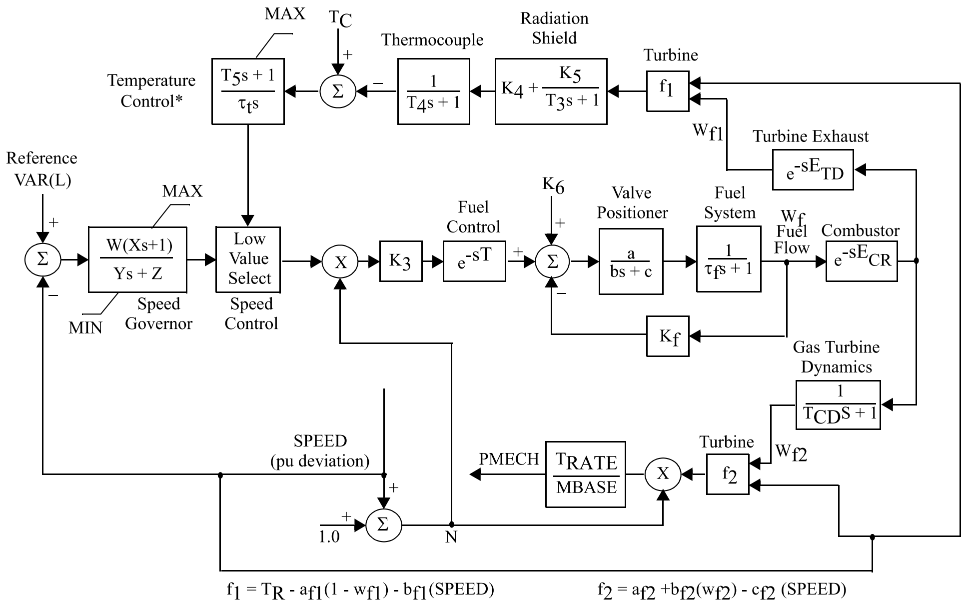

Fig. 3. GAST2 A turbine-governor dynamic model.
Source: Adopted from Siemens PTI (2010).

3. Methodology

We used the industry-standard Power System Simulator for Engineering (PSS/E) software by Siemens PTI to examine the dynamics of the future Israeli grid under changing conditions, focusing on the frequency response. The network model is comprised of both static and dynamic models, and we specify their details which are not classified as confidential information in Israel, due to national information security requirements and commercial secrets. The static model consists of hundreds of buses representing the Israeli transmission network in the year 2025, including generation units, transmission lines, loads, substations, energy storage systems (ESS) and shunt devices. The dynamic models represent the dynamics of conventional generators, utility-scale renewable energy sources (URES), loads, and energy storage systems. The dynamic models we use in this work are standard for power system studies (WECC, 2012; Pourbeik et al., 2016). However, in general, synchronous generators are modeled using the GENROU and GENSAL models, while their turbines are modeled using the TGOV and GAST family of models. Utility-scale renewable energy sources are modeled using REGCA and REECB models, and ESS are modeled using an under-frequency load shedding model, since they have a similar frequency response (Delille et al., 2012; Yang et al., 2017). Finally, the load's dependency on the frequency is modeled using a LDFRAL model. The dynamic models, as named in PSS/E, are summarized in Table 2. As an example, Fig. 3 illustrates the GAST2 A turbine-governor dynamic model as implemented in PSS/E.

The tested scenarios are constructed by modifying both the static and dynamic models with respect to their nominal values. The static model is modified to derive different scenarios of changing total demand, total renewable energy generation, conventional power dispatch, and the distribution of DRES, which are modeled as negative loads. To this end, we define a base scenario for the static model that relies on the unit commitment (UC) algorithm used by the Israel Electric Corporation for the year 2025, which represents a 14% renewable energy penetration level. This algorithm dictates in every hour of the year the total load, total renewable energy generation, power generation and consumption of pumped hydro storage systems, and the conventional power dispatch. In all scenarios we focus on the hour in

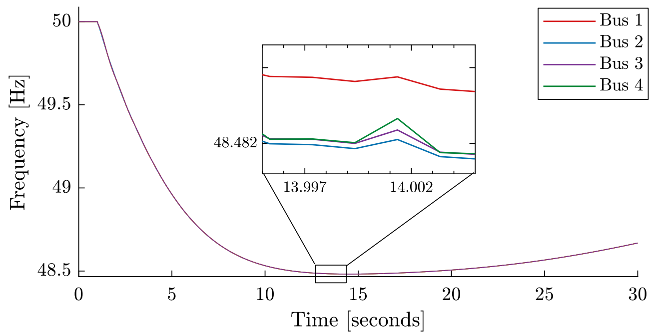

Fig. 4. Typical frequency response at four buses spread across the grid. There are no significant frequency deviations between buses at different areas.

which the ratio between the renewable energy generation and the total load is highest. The dynamic models are modified only to represent different distributions of ESS.

For each scenario we solve the power flow, simulate the loss of the largest instantaneous generation unit, and measure the frequency nadir at a large generation bus close to the center of Israel. Fig. 4 demonstrates that the frequency at a single bus represents the "system frequency" well, in the sense that there are no significant frequency deviations between buses at different areas. Note that in this study power flow constraints such as bus voltages and line loading are not closely supervised, since we assume that they do not play a major role in the dynamics that evolve following the loss of a large generation unit.

The frequency response following the loss of a large generator highly depends on the static state of the power system, and therefore it is imperative to correctly choose this state. Our strategy was to focus on the worst-case scenario. The critical moment that lead to the worst frequency response may be estimated based on two measures: the "percentage MW trip", and the instantaneous "system non-synchronous penetration ratio" (SNSP). The first is the ratio between the amount of power generation lost to the total instantaneous power generation, and the second is the instantaneous ratio between the non-synchronous power generation and the total power generation. It is well known

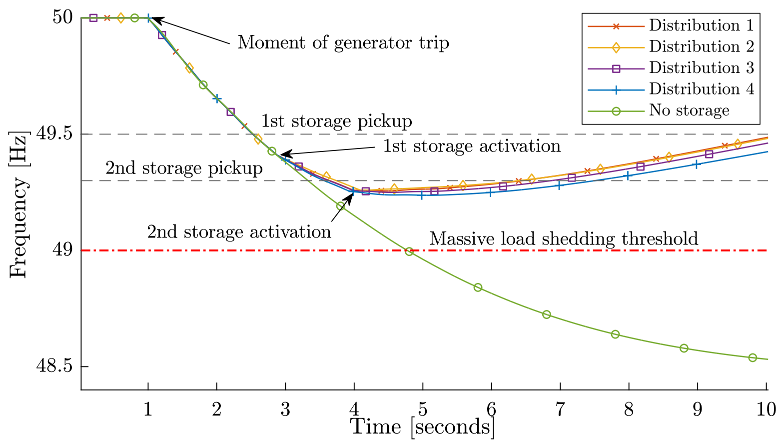

Fig. 5. Frequency response in scenario "P", with different storage distributions.

Table 3
The tested scenarios.

Examined component	Tested variable	Label	Details	
Loss of a generation unit	Unit type and location		Description	
		P	PV plant in the south	
		C	Conventional unit in the north	
Distributed RES	Geographical distribution		North [MW]	South[MW]
		South	490	1730
		Spread	790	1430
		North	1090	1130
Energy storage systems	Geographical distribution		North [MW]	South [MW]
		South	0	300
		Spread	150	150
		North	300	0
	Installation site	Loads	Loads	
		DRES	Distributed RES	
		URES	Utility-scale RES	

that high values in both measures are correlated with increased frequency deviations (Seneviratne and Ozansoy, 2016; O'Sullivan et al., 2014). Another measure that greatly impacts the frequency response is the total inertia, which generally decreases as the SNSP increases. In this study we focus on the hour (throughout the year) in which the aggregated impact of these measures should be highest, which is when the ratio between the renewable energy generation and the total load is highest, and the largest PV plant in the south is in full production.

Overall, this methodology is both scalable in terms of larger grids and relatively low on computational cost. Its scalability mostly depends on the number of regions the grid is divided to, and on the number of scenarios one wishes to examine. Due to the worst-case scenario approach, the computational cost of the proposed methodology is lower in comparison to other industry standard N-1 and N-2 reliability dynamic tests, which repeat for each of the thousands of elements in the network, and for thousands of possible scenarios. In order to have a more industry practical study that will be more extensive and will include statistical analysis then, for example, the scope of the examined scenarios can be extended. There are many ways to devise more scenarios, for example, by examining more than a single hour, or more than two generation sites for contingency.

4. Optimal distribution of renewable sources and storage units

The frequency stability of the Israeli power system is expected to be challenged as additional renewable energy sources are integrated. Currently in Israel, the integration of generation units and storage is not directed by policies that clearly consider how their distribution affects the frequency stability of the system. Rather, their distribution is usually determined by several factors such as land availability, potential energy resources, lines congestion, and environmental and economical concerns. Therefore, in this section we examine if and how the distribution of generation units and storage has an impact on the frequency response, and conclude whether appropriate policies should be implemented.

To answer these questions we study by simulations the impact of four geographical variables on the frequency response, following a loss of a large generation unit. The variables are: (1) the location and type of the lost generation unit; (2) the geographical distribution of renewable sources (DRES); (3) the geographical distribution of energy storage systems (ESS); and (4) the type of system component in which the ESS are installed. For each of these we define several scenarios, which are summarized in Table 3. Each of the scenarios is further detailed in the text below. In addition, Table 4 shows the distribution of power generation and load between north and south in scenarios "P", for the lost generation unit, and "spread", for the distribution of DRES.

Table 4
The distribution of power generation and load between north and south in scenarios "P" and "spread".

System component	North [MW]	South [MW]
Load	5830	1940
Conventional generation	900	2990
Utility-scale RES (URES)	490	1300
Distributed RES (DRES)	790	1430

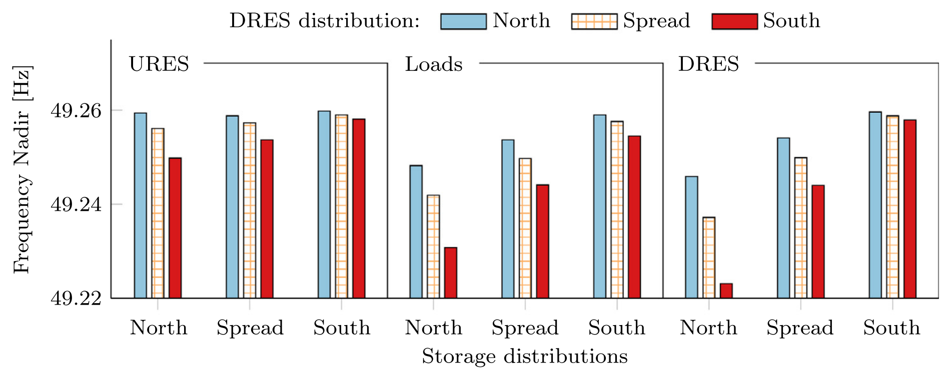

(a) Generation loss in the South.

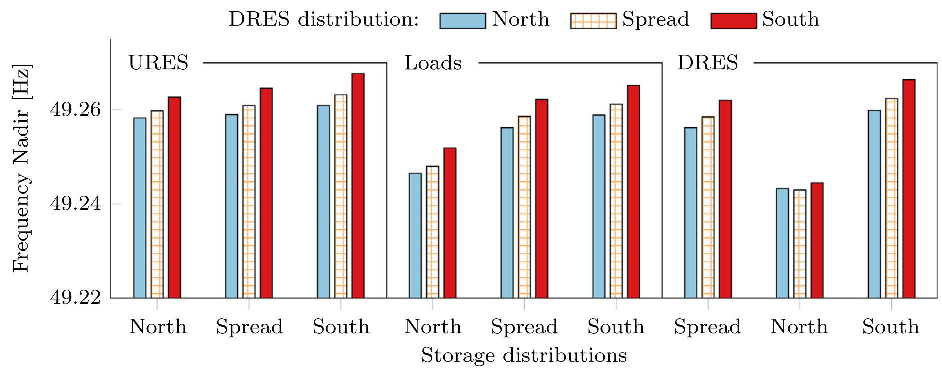

(b) Generation loss in the North.

Fig. 6. Simulation results grouped according to the geographical distribution of DRES. "Spread" distribution is as given in the IECo network model, "North" is with 300 MW of DRES moved from south to north, and in "South" they are moved from north to south.

Table 5
Frequency nadirs [Hz] following the loss of a large PV plant in the South.

Storage		Distributed RES		
Type of component	Geographical distribution	Geographical distribution		
		Spread	North	South
Utility-scale RES	Spread	49.26	49.26	49.25
	North	49.26	49.26	49.25
	South	49.26	49.26	49.26
Loads	Spread	49.25	49.25	49.24
	North	49.24	49.25	49.23
	South	49.26	49.26	49.25
Distributed RES	Spread	49.25	49.25	49.24
	North	49.24	49.25	49.22
	South	49.26	49.26	49.26

We first demonstrate how the distribution of storage affects the frequency response. Fig. 5 plots the frequency response following a loss of the large PV plant in the south (scenario "P"), in which DRES are distributed according to scenario "spread". The storage systems are distributed according to five different scenarios, as detailed in the figure. As seen in the figure, the storage systems have two levels of activation, one that starts at 49.5 Hz, and the second that starts at 49.3 Hz. The storage is activated after a delay of 150 milliseconds, after the frequency crosses the storage pickup level and remains below it for 200 milliseconds. As can be seen in the figure, the plots diverge roughly at 49.5 Hz and at 49.3 Hz when the storage systems are activated. Two main observations from this figure are: (1) storage significantly improves the frequency response; and (2) the distribution of storage has a notable effect on the frequency response.

Next, Figs. 6 to 9 present simulation results for both generation loss scenarios. Here the frequency nadir is shown for all combinations of storage and DRES distributions. In each figure the results are grouped differently in order to highlight the effects of different geographical distributions.

In Fig. 6 the results are grouped according to the three DRES distributions: "north", "south", and "spread". In the "spread" scenario DRES are distributed as given in the IECo network model for 2025. In the "north" scenario 300 MW of DRES are moved from south to north, and in the "south" scenario they are moved from north to south. As can be seen in Fig. 6(a), in case of generation loss in the south, the highest frequency nadirs are obtained with the "north" scenario, and the lowest are obtained with the "south" scenario. In addition, Fig. 6(b) shows that generation loss in the north yields contrary results, in which the highest frequency nadirs are obtained with the "south" scenario, and the lowest are obtained with the "north" scenario.

In Fig. 7 the results are grouped according to three geographical distributions of storage systems: "north", "south", and "spread". In all these scenarios 300 MW of storage are spread among buses in the system. In the "north" scenario all the storage is in the north, while in the "south" scenario it is all in the south, and in the "spread" scenario it is evenly distributed between north and south. As can be seen in the figure, in both generation loss scenarios placing storage in the south yields higher frequency nadirs, which indicate a more stable system.

In Fig. 8 the results are grouped according to three scenarios of the type of system component in which storage is installed: loads, DRES, and URES. The installed storage capacity is proportional to the power capacity of each component. As an example, when 300 MW of storage are spread across a total of 500 MW of URES, then at a single URES site of 100 MW a total of $300*(100/500) =$

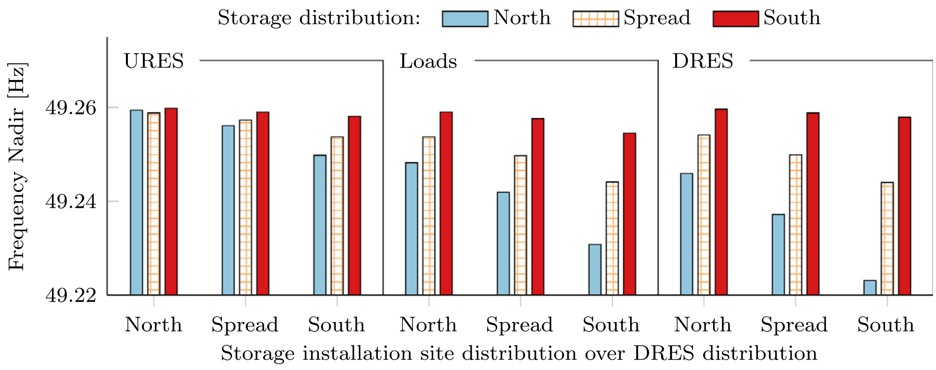

(a) Generation loss in the South.

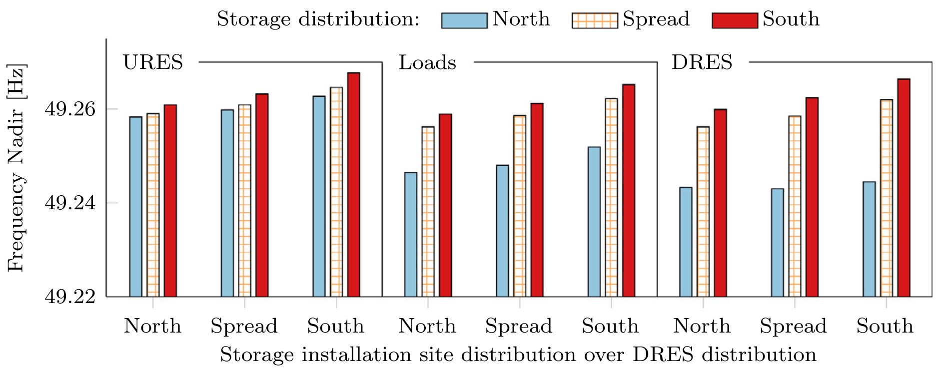

(b) Generation loss in the North.

Fig. 7. Simulation results grouped according to the geographical distribution of storage. "Spread" is for 300 MW of storage spread evenly between north and south, "North" is all 300 MW of storage in the north, and in "South" it is all in the south.

60 MW of storage will be installed. As can be seen in the figure, in both generation loss scenarios installing storage at utility-scale RES (URES) yields higher frequency nadirs.

Lastly, Fig. 9 compares the results of the two generation loss scenarios, in both a generation unit of 500 MW is disconnected from the grid. In the first scenario, labeled "P", a PV plant in the south is lost, whereas in the second scenario, labeled "C", a conventional unit in the north is lost. Scenario "P" is derived from the results of the unit commitment algorithm, in which the PV plant in the south is generating 500 MW. Scenario "C" is derived from alternating between the power dispatches of the generation units in scenario "P". The results are grouped according to the distribution of DRES. Fig. 9(a) shows the differences between the scenarios by subtracting the frequency nadirs of scenario "P" from that of scenario "C". As can be seen, scenario "C" leads to higher frequency nadirs, except when both DRES and storage are distributed in the north. Finally, Fig. 9(b) presents the minimum frequency nadir between the two scenarios. The results show that the highest frequency nadirs are obtained with the north distribution of DRES.

Table 5 lists the results of scenario "P", which according to Fig. 9(a) generally produces the worst results (lowest frequency nadirs). The frequency nadir is indicated for each combination of the three distributions of DRES, for all nine combinations of storage distributions. As can be seen, the frequency nadir ranges from 49.22 to 49.26 Hz. In addition, the maximal difference due to a change in the distribution of DRES is 20 mHz, and the maximal difference due to a change in the distribution of storage is 40 mHz.

Following are several policy recommendations that are based on these results. First the results show that the distribution of both storage and DRES have an impact on the frequency response, and that certain distributions yield better results. One conclusion is that in terms of frequency stability, storage is best placed in the south and installed at utility-scale RES (URES), as can be derived from Figs. 7 and 8. Although the results show that storage systems are better placed in URES buses, when storage is placed in the south the differences in frequency nadir are negligible. As for the distribution of DRES, Fig. 6 shows that the optimal distribution depends on the location of the lost generator, and that frequency stability improves when the DRES are placed far from this generator. In addition, from Fig. 9(b) we can resolve that in order to improve stability in the worst-case scenario, distributed RES are better placed in the north. Fig. 10 illustrates the optimal distributions, as discussed above, for the Israeli grid in 2025.

Another significant conclusion is that placing large generation units in the south poses a greater risk to frequency stability than placing them in the north. Two types of large generation units were examined: a large PV plant, and a conventional unit. The large PV plant in the south does not provide inertia nor reserves, while the conventional unit in the north does both. As a result, it is expected that the generation loss in the south will result in a better frequency response compared to the loss in the north. However, Fig. 9(a) shows that in general, losing the large generation unit in the south results in worse frequency response. Therefore, we conclude that large generation units that must be placed in the south are better placed closer to the center.

Overall, the results above show that storage is better placed in the south, and generation units in the north. This general conclusion may stem from two unique properties of the Israeli grid: (1) its isolated nature, which makes its dynamic behavior more sensitive; and (2) the geographical distribution of generation units, which results in less inertia in the south. As seen in

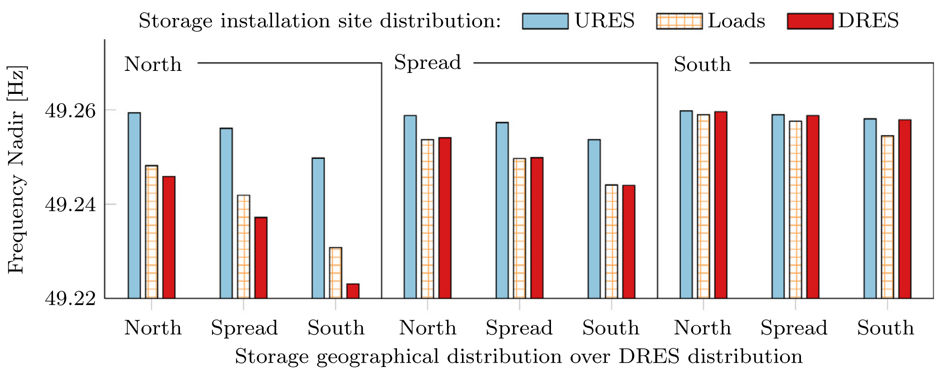

(a) Generation loss in the South.

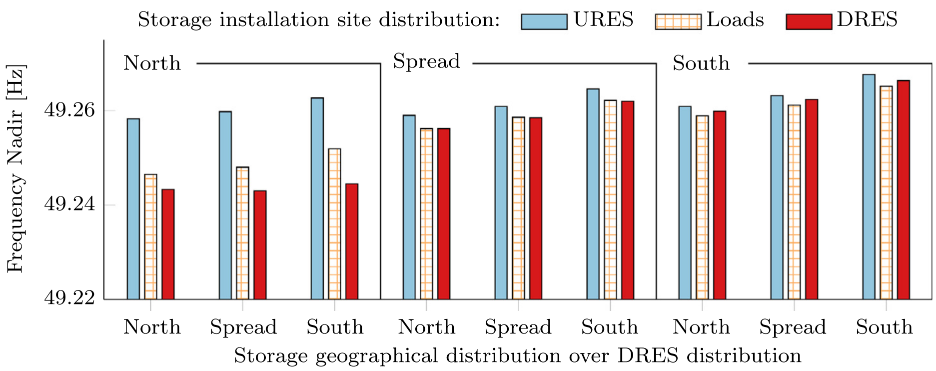

(b) Generation loss in the North.

Fig. 8. Simulation results grouped according to the type of system component in which storage is installed.

Fig. 1, most of the conventional generation is in the south but very close to the center of Israel, while the inertia-less generation of renewable energy sources is predominately deeper in the south. Moreover, most of the load is located in the center-north, and so if our model took into account the inertia of the loads, then the results would have probably been even more conclusive.

The optimal distribution of generation units partly matches the available land in Israel. In the north, where available land is scarce, distributed RES may be installed using a dual-purpose approach on existing infrastructure, such as on rooftops and water reservoirs. However, although the south of Israel has more available land and higher solar potential, placing large renewable energy sources in this area increases the risk for frequency instability. Still, it should be more economic and sustainable to place them in this area, and to maintain a stable frequency by employing other strategies and policies, such as demand response and spinning reserve regulation. Moreover, it is estimated that in order to reach the renewable energy target of 2030, large renewable energy sources must be placed in the available land in the south, as there is little land available in other regions of Israel (Israel Electric Authority, 2020a).

Although the geographical distribution of both storage and DRES impact the frequency response, we conclude that the impact of the first is significantly greater than the second. This is implied by the differences between the geographical distribution scenarios and their impact on the frequency response. As can be seen in Table 3, the difference in power capacity between the geographical distribution scenarios of DRES is double than between those of storage (300 MW vs. 150 MW). However, Table 5 shows that the maximum difference due to a change in the distribution of storage is about twice as the difference due to a change in the distribution of DRES (40 mHz vs. 20 mHz). This may imply that policy makers should prioritize storage distribution policies over DRES distribution policies.

5. Storage requirements for frequency stability

Recently, the Israeli renewable energy penetration target for 2030 was dramatically increased from 17% to 30%. This means that in 2025 the renewable energy penetration level is expected to be higher than the planned target of 13%. These high targets, and the periods of high shares of renewable energy already experienced in the Israeli grid in 2020 (Carmon et al., 2020), raises concerns related to frequency stability. A central question is what amount of storage is required to maintain stability, and how storage devices should be deployed in the grid. In this section we attempt to answer two more specific questions. The first is what is the minimal storage power that is required for maintaining stability in typical scenarios. In this context, we define the minimal storage power as the power needed to prevent the frequency from falling under 49 Hz, which is the threshold for massive load shedding. The second question is how sensitive the frequency response is to changes in available storage power.

The scenarios in this section are based on the scenarios described in Section 4. For a lose of generation unit we examine scenario "P", which is more realistic as it is derived from the IECo unit commitment algorithm, and for the distribution of DRES we use scenario "spread", to eliminate the effect of the distribution of DRES. For storage we examine multiple combinations of scenarios, where each combination includes one of three renewable energy penetration targets, 14%, 17%, and 20%, and one of 10 storage capacity values, ranging roughly from 100 MW to 300 MW. The conventional power dispatch assumes a 14% penetration level of renewables, and is derived from the unit commitment algorithm used by the IECo. The power dispatch in higher targets is derived from a process in which we modify the

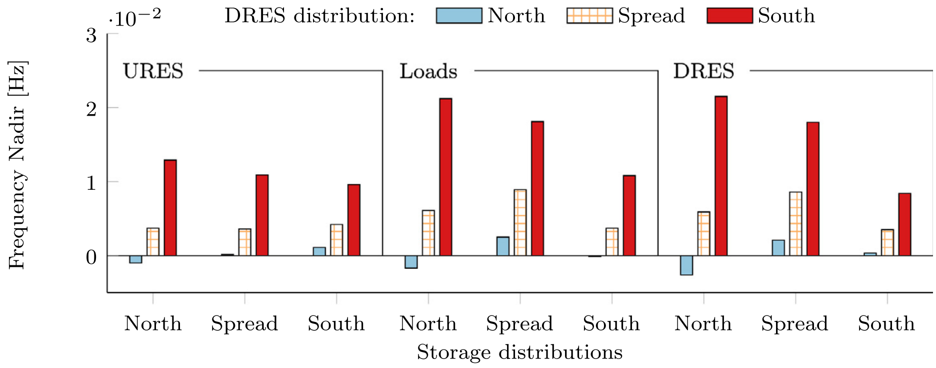

(a) Frequency nadirs of scenario "C" minus those of scenario "P".

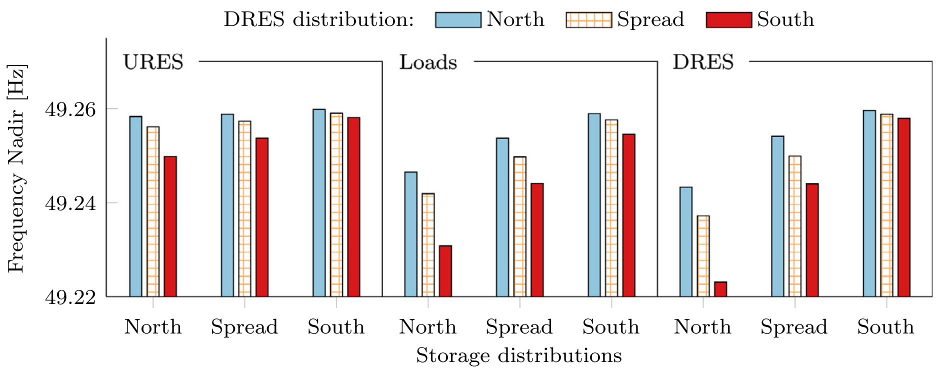

(b) Minimum frequency nadirs between scenarios "C" and "P".

Fig. 9. Comparison of frequency nadirs between the generation loss scenarios. Scenario "P" is for a loss of a 500 MW PV plant in the south, whereas scenario "C" is for the same power loss but in a conventional unit in the north.

14% dispatch to include more power from DRES on account of power from conventional units.[3]

Based on our model, at the 20% renewable energy penetration target the system reaches a conventional generation must-run limit. At this limit the online steam units operate at their minimum allowed power, and all other conventional generation units, except for co-generation units, are disconnected. According to the unit commitment algorithm, the steam units operate before and after the examined hour and cannot be turned off and on rapidly, while the co-generation units supply power as part of industrial processes, and therefore are not controlled by the TSO during normal operation. A general example of this daily process is illustrated in Fig. 11, in which the must-run limit is achieved at an instantaneous renewable energy penetration level of 60%.

Figs. 12 and 13 present the results for the best and worst storage distributions as analyzed in Section 4, for several storage capacities, and for different renewable energy penetration levels. Fig. 12 illustrates the frequency nadirs with respect to storage power capacity. The markers represent the simulation results, and the continuous lines are fitted quadratic functions. Fig. 13 plots the derivatives of these fitted functions, and thus illustrates the sensitivity of the frequency nadir to the total storage power. The resulting sensitivity ranges from 3 mHz/MW at 140 MW to 1 mHz/MW at 300 MW.

Table 6 presents the minimal storage power requirements for which the frequency nadir reaches the 49 Hz threshold of massive load shedding. The results are given for the different distributions of storage systems which are installed either all in the south or the north, and at URES, DRES, or loads. The table also lists in parentheses the ratio between the required storage power capacity and the installed power capacity at a certain location, namely the "MW storage per MW installed" (MSMI) measure. For instance, a 146 MW storage device installed alongside a total load of 5840 MW will result in MSMI = 146/5840 = 0.025. As can be seen, the storage requirements ranges from 140 to 190 MW, and the maximal difference between north and south for each target is up to 14 MW. The MSMI ranges from 0.025 to 0.361, where the highest value is obtained when installing storage at URES sites in the north, and the lowest value is obtained when installing storage near loads in the north.

Following is a general discussion and several policy recommendations that stem from the results above. First we find that Israel today already has the required energy storage power capacity to maintain frequency stability, considering a loss of a large generation unit in 2025, and assuming 14%, 17%, or 20% renewable energy penetration levels. Table 6 shows that no more than 190 MW of storage will be required for these penetration levels. This requirement for storage can be fulfilled by the existing 300 MW pumped hydro storage (PHS) system, that also supports

Table 6
Minimal storage power requirements and MSMI (in parentheses) for different distributions of storage systems. Extreme values are in bold.

Target	Area	URES [MW]	DRES [MW]	Loads [MW]
14%	North	149(.304)	160(.202)	157(.027)
	South	147(.139)	146(.102)	147(.080)
17%	North	141(.288)	149(.138)	146(**.025**)
	South	143(.135)	**140**(.072)	141(.077)
20%	North	177(**.361**)	**190**(.139)	189(.033)
	South	188(.177)	186(.075)	184(.100)

[3] It should be noted that this dispatch process is not the standard dispatch process in which the unit commitment algorithm is re-executed for each target.

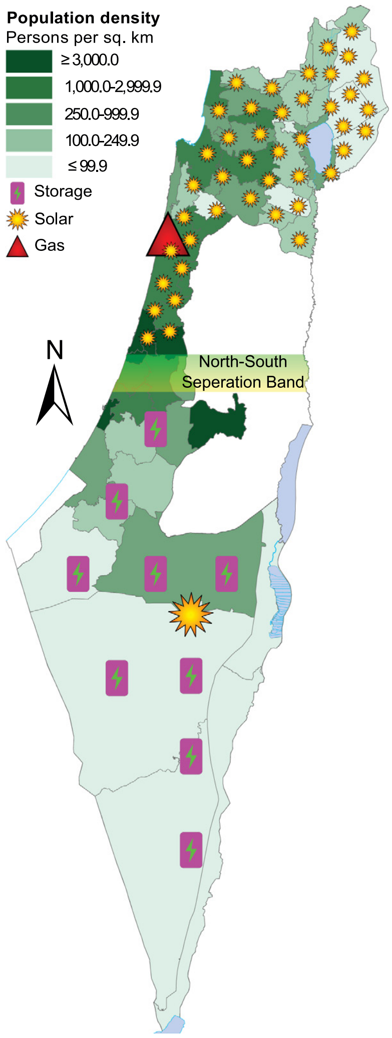

Fig. 10. Optimal storage and DRES distributions for frequency stability, following a loss of a large generator in the 2025 Israeli grid.

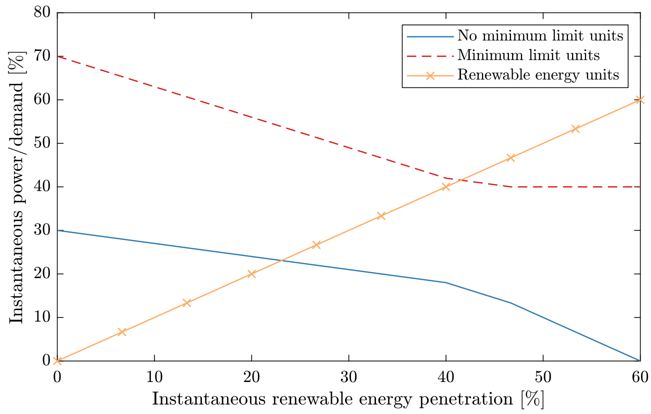

Fig. 11. Example of power distribution between different types of units, based on the must-run limit. At this limit the online steam units operate at their minimum allowed power, and all other conventional generation units, except for co-generation units, are disconnected.

automatic load shedding, but only when the storage is charging (Shikun Binui, Electra, 2016). Charging the storage system also increases the load, the generation, and the inertia in the grid, all of which has a positive effect on frequency stability.

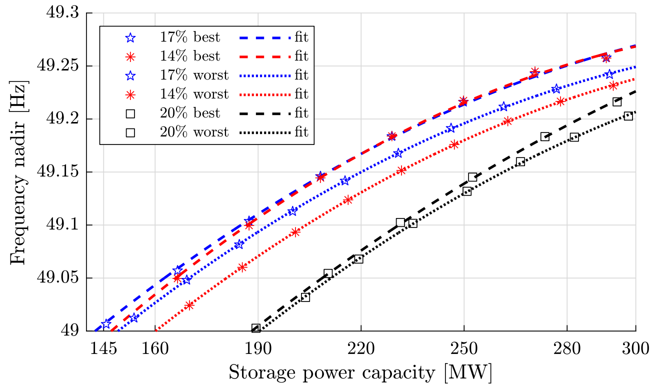

Fig. 12. Frequency nadir as a function of storage power (markers), and quadratic fitting (dotted lines) for different renewable energy penetration levels, and for the best-case and worst-case storage distributions.

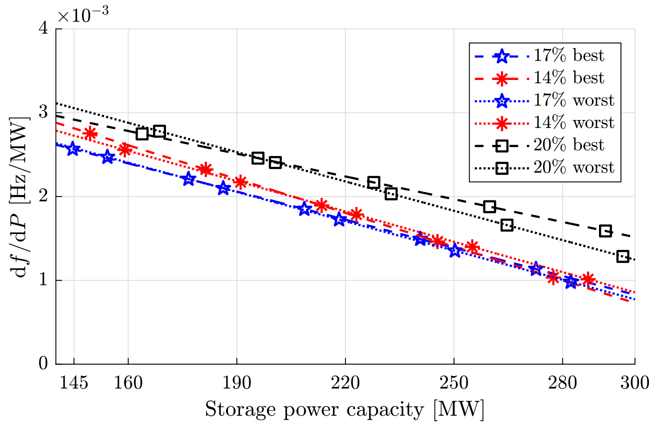

Fig. 13. Derivatives of the quadratic fitting functions from Fig. 12.

Because this existing pumped hydro storage system provides sufficient capabilities for frequency stability only in charging operation, policy makers should encourage that this and additional storage systems will be available for frequency regulation when there is a risk of instability. In this light, until 2025 two more PHS systems and at least 168 MW of distributed PV plus storage will be connected to the grid (Israel Electric Authority, 2020c,b). Nevertheless, the contribution of these additional storage systems to the frequency regulation in case of a large disturbance is currently limited, for two main reasons: (1) frequency regulation policies for these storage systems are not yet defined; (2) storage in PV sites is expected to store excess renewable energy that cannot be injected to the grid, and thus cannot impact the power balance following a disturbance. In the future, increasing the power capacity of these storage systems may allow them to participate in frequency regulation.

In addition, our results show that storage requirements do not change monotonically with renewable energy penetration targets. According to Table 6, storage capacity requirements *decrease* when moving from 14% to 17% penetration level, and *increase* when moving from 17% to 20%. This result can be explained based on the dispatch process: when increasing the renewable energy penetration level from 14% to 17% the number of conventional units do not change, so the system inertia remains constant, but the spinning reserve increases, which leads to higher operational flexibility. However at 20% penetration the must-run limit dictates that several conventional generation units must be shutdown, and as a result the total system inertia is reduced, which has an adverse effect on frequency response. This may indicate that although higher operational flexibility can be an alternative to storage, the last should be preferred since there are times when flexibility is limited, for example when reaching the must-run limit.

Another issue is the crucial timing of storage systems integration. For instance, in order to postpone the need for storage, large renewable energy sources that lack inertia should be integrated in specific seasons of the year. These seasons are characterized by high demand and stable production of renewable energy, which reduce the risk for frequency instability. In other seasons in which the risk for instability is higher, sufficient storage or flexible operation strategies should be already available. In Israel, according to measurements of load and solar generation, the season which poses the greatest risk for instability is the spring when the load is minimal and the solar generation is maximal, whereas during the summer and the winter this risk is minimal as either the load maximizes or solar generation minimizes. In this light, it may be best to time the connection of the planned 500 MW PV plant in the south to the summer. This will allow maximum time to prepare sufficient storage systems until the following spring.

Furthermore, the measure of MW storage per MW installed (MSMI), presented in Table 6, may indicate how the distribution of storage can affect energy curtailment. Such curtailment might occur at buses that contain both renewable energy sources and storage systems, when excess generated energy cannot be stored nor injected into the grid. Normally this will occur when the storage is full, and the output of the renewable energy sources is greater than the load at the bus plus the bus connection limit. If the storage is also used for frequency regulation then additional energy must be curtailed, since for the storage to provide its allocated power for frequency regulation there must be a gap between the net output power at the bus and the connection limit. The size of this gap can be calculated by multiplying the MSMI by the installed power of the RES in each bus.

The results also show that the marginal contribution of storage for frequency regulation decreases as the overall power capacity of storage devices in the grid increases. It is obvious that higher storage power capacity leads to higher frequency nadir. However, as seen in Figs. 12 and 13, for higher values of storage power capacity the relative increase in frequency nadir is smaller.

6. Conclusions and policy implications

In this study we explore how the location and size of renewable energy sources and energy storage systems impact the frequency stability of the grid as we focus on Israel in 2025, using the most realistic dynamic model available. Other countries that wish to learn from this study can either use similar methodology, estimate their results based on ours, or discuss whether they can reach similar or contrary conclusions and policy recommendations.

Based on simulation results, our main conclusions and policy recommendations are as follows:

- Israel today can maintaining a stable frequency in 2025, considering the examined power dispatches and renewable energy penetration levels, using the existing pumped hydro storage system but only during charging operation.
- In this light, to maintain a reliable system, policy makers should encourage, probably through legislation, that the existing and additional storage systems will be available for frequency regulation.
- Storage requirements do not change monotonically with renewable energy penetration targets, probably as a result of increasing flexibility until a must-run limit is reached at which the system inertia declines.
- Until sufficient storage systems will be deployed and relevant policies will be declared, operating the system with high flexibility can support the desired targets of renewable energy integration.
- We suggest a measure named "MW storage per MW installed" (MSMI), that indicates how the distribution of storage may affect energy curtailment at buses that contain both renewable energy sources and storage systems.
- The location of renewable energy sources and energy storage systems has an impact on the frequency stability, and their preferred location seems to balance the distribution of inertia in the Israeli grid.
- However, we conclude that this impact is not yet strong enough to be a leading factor in determining the location of these sources in Israel at least until 2025. This is because there are other more challenging technical considerations with economical influences much stronger than those of the different strategies to maintain frequency stability. These considerations mainly include land availability and solar potential that are mandatory to reach Israel's renewable energy targets. As explained in Section 2.2 and demonstrated in Fig. 2, in the south there is high PV potential as well as low-cost and available land. Moreover, in Section 4 we present the claim that it is estimated that in order to reach the renewable energy target of 2030, large renewable energy sources must be placed in the available land in the south, as there is little land available in other regions of Israel.
- Furthermore, we estimate that after 2025 this impact will diminish due to a more homogeneous distribution of inertia in the likely scenario that storage systems will be placed adjacent to renewable energy sources in the south, and that these systems will provide inertial services. We believe it is the likely scenario as we see research and industry trends to co-locate energy storage systems and renewable energy sources for capacity firming (IEA, 2020), and to implement inertial services in such inverter based resources (Matevosyan et al., 2019). On the other hand, we estimate that this impact would be stronger if the placement and functions of these resources will further emphasize the heterogeneous distribution of inertia.

CRediT authorship contribution statement

Gefen Ben Yosef: Conceptualization, Methodology, Software, Validation, Formal analysis, Investigation, Writing – original draft, Writing – review & editing, Visualization, Project administration. **Aviad Navon:** Writing – original draft, Writing – review & editing. **Olga Poliak:** Conceptualization, Methodology, Validation, Resources, Writing – review & editing. **Naomi Etzion:** Writing – review & editing. **Nurit Gal:** Writing – review & editing. **Juri Belikov:** Visualization. **Yoash Levron:** Conceptualization, Writing – review & editing, Supervision, Project administration, Funding acquisition.

Declaration of competing interest

The authors declare that they have no known competing financial interests or personal relationships that could have appeared to influence the work reported in this paper.

Acknowledgment

This research was partly supported by the Israel Ministry of Energy, grant no. 218-11-034, and by the Israel Science Foundation, grant no. 1227/18.

References

Abdlrahem, A., Venayagamoorthy, G.K., Corzine, K.A., 2013. Frequency stability and control of a power system with large PV plants using PMU information. In: 2013 North American Power Symposium (NAPS). pp. 1–6. http://dx.doi.org/10.1109/NAPS.2013.6666929.

Adrees, A., Milanovic, J.V., 2016. Study of frequency response in power system with renewable generation and energy storage. In: 2016 Power Systems Computation Conference (PSCC). pp. 1–7. http://dx.doi.org/10.1109/PSCC.2016.7540912.

Alquthami, T., Ravindra, H., Faruque, M.O., Steurer, M., Baldwin, T., 2010. Study of photovoltaic integration impact on system stability using custom model of PV arrays integrated with PSS/E. In: North American Power Symposium 2010. pp. 1–8. http://dx.doi.org/10.1109/NAPS.2010.5619589.

Bawazir, R.O., Cetin, N.S., 2020. Comprehensive overview of optimizing PV-DG allocation in power system and solar energy resource potential assessments. Energy Rep. 6, 173–208. http://dx.doi.org/10.1016/j.egyr.2019.12.010.

Bogdanov, D., Breyer, C., 2015. The role of solar energy towards 100% renewable power supply for Israel: Integrating solar PV, wind energy, CSP and storages. In: Proceedings of the 19th Sede Boqer Symposium on Solar Electricity Production February 23-25, 2015. pp. 1–4.

Carmon, D., Navon, A., Machlev, R., Belikov, J., Levron, Y., 2020. Readiness of small energy markets and electric power grids to global health crises: Lessons from the COVID-19 pandemic. IEEE Access 8, 127234–127243. http://dx.doi.org/10.1109/ACCESS.2020.3008929.

Cheema, K.M., Mehmood, K., 2020. Improved virtual synchronous generator control to analyse and enhance the transient stability of microgrid. IET Renew. Power Gener. 14 (4), 495–505. http://dx.doi.org/10.1049/iet-rpg.2019.0855.

Delille, G., Francois, B., Malarange, G., 2012. Dynamic frequency control support by energy storage to reduce the impact of wind and solar generation on isolated power system's inertia. IEEE Trans. Sustain. Energy 3 (4), 931–939. http://dx.doi.org/10.1109/TSTE.2012.2205025.

Halász, G., Malachi, Y., 2014. Solar energy from negev desert, Israel: Assessment of power fluctuations for future PV fleet. Energy Sustain. Dev. 21, 20–29. http://dx.doi.org/10.1016/j.esd.2014.04.005.

Hirth, L., Ziegenhagen, I., 2015. Balancing power and variable renewables: Three links. Renew. Sustain. Energy Rev. 50, 1035–1051. http://dx.doi.org/10.1016/j.rser.2015.04.180.

IEA, 2020. Energy storage. [Online] Available https://www.iea.org/reports/energy-storage, Accessed September 5, 2021.

Israel Central Bureau of Statistics, 2019. Population density by natural regions 2018. [Online] Available https://www.cbs.gov.il/he/publications/doclib/2019/2.shnatonpopulation/02_01e.pdf, Accessed January 30, 2020.

Israel Electric Authority, 2019. Electricity market report for 2018. [Online] Available https://www.gov.il/he/Departments/General/dochmeshek, Accessed August 9, 2020.

Israel Electric Authority, 2020a. Increasing 2030 targets of electricity production from renewable energy. [Online] Available https://www.gov.il/BlobFolder/reports/2030_final/he/General_2030_eng.pdf, Accessed October 3, 2020.

Israel Electric Authority, 2020b. Press release results for PV plus storage tender. [Online] Available https://www.gov.il/he/departments/news/pv_agira, Accessed July 30, 2020.

Israel Electric Authority, 2020c. Transmission network licenses. [Online] Available https://www.gov.il/BlobFolder/reports/statusrish/he/Files_Rishyonot_mutnim_07_2020.pdf, Accessed September 29, 2020.

Israel Government Portal, 2017. Meteorological service database. [Online] Available https://ims.data.gov.il, Accessed July 30, 2020.

Israel Ministry of Energy, 2020. Policy principles increasing 2030 targets of electricity production from renewable energy. [Online] Available https://www.gov.il/he/departments/policies/elecricity_aug_2020, Accessed August 14, 2020.

Israel Prime Ministers Office, 2015. Israel government decision 542 greenhouse gas emission reduction and efficiency improvement of the national energy consumption. [Online] Available https://www.gov.il/he/Departments/policies/2015_dec542, Accessed April 23, 2019.

Kottick, D., Blau, M., Edelstein, D., 1993. Battery energy storage for frequency regulation in an island power system. IEEE Trans. Energy Convers. 8 (3), 455–459. http://dx.doi.org/10.1109/60.257059.

Kottick, D., Blau, M., Winokur, M., 1991. An introduction to dynamic security of supply in the Israeli power system. In: 17th Convention of Electrical and Electronics Engineers in Israel. pp. 338–341. http://dx.doi.org/10.1109/EEIS.1991.217700.

Liang, X., 2017. Emerging power quality challenges due to integration of renewable energy sources. IEEE Trans. Ind. Appl. 53 (2), 855–866. http://dx.doi.org/10.1109/TIA.2016.2626253.

Liu, Y., You, S., Tan, J., Zhang, Y., Liu, Y., 2018. Frequency response assessment and enhancement of the U.S. power grids toward extra-high photovoltaic generation penetrations—an industry perspective. IEEE Trans. Power Syst. 33 (3), 3438–3449. http://dx.doi.org/10.1109/TPWRS.2018.2799744.

Matevosyan, J., Badrzadeh, B., Prevost, T., Quitmann, E., Ramasubramanian, D., Urdal, H., Achilles, S., MacDowell, J., Huang, S.H., Vital, V., O'Sullivan, J., Quint, R., 2019. Grid-forming inverters: Are they the key for high renewable penetration? IEEE Power Energy Mag. 17 (6), 89–98. http://dx.doi.org/10.1109/MPE.2019.2933072.

Mentesidi, K., Khallaayoun, A., Harmouch, F.Z., Loudiyi, K., Aguado, M., 2016. PV and CSP integration study experience in a Mediterranean partner country. IET Renew. Power Gener. 10 (1), 42–49. http://dx.doi.org/10.1049/iet-rpg.2015.0142.

Milano, F., Dörfler, F., Hug, G., Hill, D.J., Verbic, G., 2018. Foundations and challenges of low-inertia systems (invited paper). In: 2018 Power Systems Computation Conference (PSCC). pp. 1–25. http://dx.doi.org/10.23919/PSCC.2018.8450880.

Navon, A., Kulbekov, P., Dolev, S., Yehuda, G., Levron, Y., 2020. Integration of distributed renewable energy sources in Israel: Transmission congestion challenges and policy recommendations. Energy Policy 140, 111412. http://dx.doi.org/10.1016/j.enpol.2020.111412.

O'Sullivan, J., Rogers, A., Flynn, D., Smith, P., Mullane, A., O'Malley, M., 2014. Studying the maximum instantaneous non-synchronous generation in an island system—Frequency stability challenges in Ireland. IEEE Trans. Power Syst. 29 (6), 2943–2951. http://dx.doi.org/10.1109/TPWRS.2014.2316974.

Poolla, B.K., Bolognani, S., Dörfler, F., 2017. Optimal placement of virtual inertia in power grids. IEEE Trans. Automat. Control 62 (12), 6209–6220. http://dx.doi.org/10.1109/TAC.2017.2703302.

Poolla, B.K., Groß, D., Dörfler, F., 2019. Placement and implementation of grid-forming and grid-following virtual inertia and fast frequency response. IEEE Trans. Power Syst. 34 (4), 3035–3046. http://dx.doi.org/10.1109/TPWRS.2019.2892290.

Pourbeik, P., Agrawal, B., Patterson, S., Rhinier, R., Energy, D., 2016. Modeling of synchronous generators in power system studies. Cigre Sci. Eng. 6, 21–32, [Online] Available https://e-cigre.org/publication/CSE006-cse-006.

Pulgar-Painemal, H., Wang, Y., Silva-Saravia, H., 2018. On inertia distribution, inter-area oscillations and location of electronically-interfaced resources. IEEE Trans. Power Syst. 33 (1), 995–1003. http://dx.doi.org/10.1109/TPWRS.2017.2688921.

Remon, D., Cantarellas, A.M., Mauricio, J.M., Rodriguez, P., 2017. Power system stability analysis under increasing penetration of photovoltaic power plants with synchronous power controllers. IET Renew. Power Gener. 11 (6), 733–741. http://dx.doi.org/10.1049/iet-rpg.2016.0904.

Seneviratne, C., Ozansoy, C., 2016. Frequency response due to a large generator loss with the increasing penetration of wind/PV generation – A literature review. Renew. Sustain. Energy Rev. 57, 659–668. http://dx.doi.org/10.1016/j.rser.2015.12.051.

Shikun Binui, Electra, 2016. Gilboa pumped hydro storage technical report. [Online] Available https://events.eventact.com/Ortra/20451/project_titel.pdf, Accessed September 29, 2020.

Siemens PTI, 2010. PSS/E 32.0.5 model library.

Silva-Saravia, H., Pulgar-Painemal, H., Mauricio, J.M., 2017. Flywheel energy storage model, control and location for improving stability: the Chilean case. IEEE Trans. Power Syst. 32 (4), 3111–3119. http://dx.doi.org/10.1109/TPWRS.2016.2624290.

Singh, B., Mishra, D.K., 2018. A survey on enhancement of power system performances by optimally placed DG in distribution networks. Energy Rep. 4, 129–158. http://dx.doi.org/10.1016/j.egyr.2018.01.004.

Solomon, A., Bogdanov, D., Breyer, C., 2019. Curtailment-storage-penetration nexus in the energy transition. Appl. Energy 235, 1351–1368. http://dx.doi.org/10.1016/j.apenergy.2018.11.069.

Solomon, A., Faiman, D., Meron, G., 2010. An energy-based evaluation of the matching possibilities of very large photovoltaic plants to the electricity grid: Israel as a case study. Energy Policy 38 (10), 5457–5468. http://dx.doi.org/10.1016/j.enpol.2009.12.024.

Solomon, A., Faiman, D., Meron, G., 2012a. Appropriate storage for high-penetration grid-connected photovoltaic plants. Energy Policy 40, 335–344. http://dx.doi.org/10.1016/j.enpol.2011.10.019.

Solomon, A., Faiman, D., Meron, G., 2012b. The role of conventional power plants in a grid fed mainly by PV and storage, and the largest shadow capacity requirement. Energy Policy 48, 479–486. http://dx.doi.org/10.1016/j.enpol.2012.05.050.

Tahir, M.F., Haoyong, C., Khan, A., Javed, M.S., Laraik, N.A., Mehmood, K., 2019a. Optimizing size of variable renewable energy sources by incorporating energy storage and demand response. IEEE Access 7, 103115–103126. http://dx.doi.org/10.1109/ACCESS.2019.2929297.

Tahir, M.F., Haoyong, C., Mehmood, K., Ali, N., Bhutto, J.A., 2019b. Integrated energy system modeling of China for 2020 by incorporating demand response, heat pump and thermal storage. IEEE Access 7, 40095–40108. http://dx.doi.org/10.1109/ACCESS.2019.2905684.

Ulbig, A., Borsche, T.S., Andersson, G., 2014. Impact of low rotational inertia on power system stability and operation. IFAC Proc. Vol. 47 (3), 7290–7297. http://dx.doi.org/10.3182/20140824-6-ZA-1003.02615.

Vardimon, R., 2011. Assessment of the potential for distributed photovoltaic electricity production in Israel. Renew. Energy 36 (2), 591–594. http://dx.doi.org/10.1016/j.renene.2010.07.030.

WECC, WECC Renewable Energy Modeling Task Force, 2012. Generic solar photovoltaic system dynamic simulation model specification. [Online] Available https://www.powerworld.com/files/WECC-Solar-PV-Dynamic-Model-Specification-September-2012.pdf, Accessed October 12, 2020.

Wu, Y., Tsai, S., Zou, M., 2013. Accommodating high PV penetration on the distribution system of Kinmen island. Energy Power Eng. 05 (04), 209–214. http://dx.doi.org/10.4236/epe.2013.54b041.

Wu, Y., Ye, G., Shaaban, M., 2016. Analysis of impact of integration of large PV generation capacity and optimization of PV capacity: case studies in Taiwan. IEEE Trans. Ind. Appl. 52 (6), 4535–4548. http://dx.doi.org/10.1109/TIA.2016.2594283.

Yang, D., Liu, S., Cai, G., 2017. Optimal system frequency response model and UFLS schemes for a small receiving-end power system after islanding. Appl. Sci. 7 (5), 468. http://dx.doi.org/10.3390/app7050468.